Synthesis and Reactivity of Aza-Capped Encapsulated Co(III) Ions

I. I. Creaser, R. J. Geue, J. MacB. Harrowfield, A. J. Herlt, A. M. Sargeson,* M. R. Snow, and J. Springborg

Contribution from the Research School of Chemistry, Australian National University, Canberra, ACT 2600, and the Department of Physical and Inorganic Chemistry, University of Adelaide, Adelaide, SA, Australia. *Received August 7, 1981*

Abstract: The synthesis of the cage complexes $[Co(sep)]^{2+/3+}$ from $[Co(en)_3]^{3+}$ (sep = sepulchrate = 1,3,6,8,10,13,16,19-octaazabicyclo[6.6.6]eicosane) and analogous cages from $[Co(sen)]^{3+}$ (sen = 5-methyl-5-(4-amino-2-azabutyl)-3,7-diazanonane-1,9-diamine) are described, and the crystal structure of $[Co(sep)]S_2O_6 \cdot H_2O$ is reported. The oxidation-reduction potentials, visible spectra, rotary dispersion, circular dichroism, and magnetism of the Co(II)-Co(III) oxidation states are recorded, along with the acid-base properties and stability of the cages toward acids and bases. The Co(II)-Co(III) electron self-exchange rates are unusually fast (5.1 and 2.9 M^{-1} s^{-1} at 25 °C) and $\sim 10^5$-fold greater than that for $[Co(en)_3]^{3+/2+}$. The $[Co(sep)]^{2+}$ reduction of O_2 to H_2O_2 is also rapid (43 M^{-1} s^{-1} at 25 °C) and apparently occurs by an outer-sphere path rather than through the route that leaves O_2^{2-} bound to two Co(III) ions. The complexes are unusually stable, and the chemistry is unusual for Co(II)-Co(III) systems.

The synthesis of large fused-ring systems like the cryptates in which the entropy effects for ring closure are unfavorable requires rather sophisticated methods.[1] One way to overcome the problem is to do the organic chemistry around a metal ion so that the large ring synthesis can be reduced to several small ring syntheses, and this strategy has been applied to the synthesis of two nitrogen analogues of the polyether cryptates. The results of some of the experiments described in this paper have already appeared in a short communication.[2]

Experimental Section

All chemicals were analytical grade. Commercial CF_3SO_3H (3M Co.) was distilled before use. CF_3SO_3Li was prepared from Li_2CO_3 and CF_3SO_3H.

^1H NMR spectra were recorded with a JEOL 100-MHz Minimar spectrometer at 30 °C relative to tetramethylsilane as an external standard, and ^{13}C NMR spectra were recorded with a JEOL JNM-FX 60 Fourier transform NMR spectrometer at 25 °C relative to 1,4-dioxane as an internal standard. Chemical shifts are reported as positive downfield from the references and negative upfield.

Cary 118 and 16 K spectrophotometers were used for the absorption spectra and kinetic runs. Optical rotations were measured with a Perkin-Elmer P 22 spectropolarimeter, and circular dichroism measurements were made with a JASCO Model RD/UV instrument incorporating the Sproul Scientific SS 20 CD modification. Cyclic voltammetry measurements were performed by using a three-electrode *iR*-compensated system with a platinum auxiliary electrode and PAR Model 170 instrumentation. Magnetic susceptibilities were measured by the Gouy and Faraday methods on a Newport Instruments single-temperature Gouy balance with solid $[Ni(en)_3]S_2O_6$ as the calibrant.

All oxygen-sensitive experiments were performed in an atmosphere of pure nitrogen or argon after the gases had been scrubbed with solutions of Cr^{2+}.

All evaporations were carried out with Büchi rotary evaporators at ~15-mmHg pressure so that the temperature of the solution did not exceed 25 °C.

Synthesis of [(1,3,6,8,10,13,16,19-Octaazabicyclo[6.6.6]eicosane)cobalt(III)] Chloride ([Co(sep)]Cl$_3$). To a stirred suspension of Li_2CO_3 (25 g) and (±)-$[Co(en)_3]Cl_3 \cdot H_2O$ (18.2 g, 0.05 mol) in water (125 mL) were added 27% aqueous ammonia (166 mL, 2.5 mol) diluted to 592 mL and 36% aqueous formaldehyde (592 mL, 7.5 mol). The solutions were added separately and continuously over 2 h by using a peristaltic pump. The mixture was stirred for another 0.5 h, the Li_2CO_3 filtered off, and the pH of the filtrate adjusted to ~3 with concentrated $HClO_4$. The solution was sorbed on an ion-exchange column (Dowex 50W-X2, 200-400 mesh, H^+ form, 5 × 10 cm). The column was eluted with trisodium citrate (5 L of 0.2 M) to remove a pink species, which was discarded. The resin bed was then washed with H_2O and 1 M HCl to remove Na^+ and the orange species removed from the column by eluting with HCl (3 M, ~3 L). The eluate was taken down to dryness on a vacuum evaporator at 50 °C. The isolated compound was recrystallized by dissolving it in water (90 °C) and adding acetone dropwise while cooling in an ice bath and stirring (yield 16.7 g, 74%). Anal. Calcd for $CoC_{12}N_8H_{30}Cl_3$: Co, 13.05; C, 31.91; N, 24.81; H, 6.69; Cl, 23.54. Found: Co, 12.9; C, 31.3; N, 25.5; H, 7.1; Cl, 22.8.

Synthesis of [Co(sep)]ZnCl$_4$·H$_2$O. A solution of $[Co(sep)]Cl_3$ (1.0 g) in water (50 mL) (flushed with nitrogen to remove all dissolved oxygen) was added to an oxygen-free suspension of Zn dust (~1 g) in water (10 mL). The reduction took place within seconds, producing a pale yellow solution. The Zn dust was filtered off under nitrogen, an ice-cold solution of an oxygen-free solution of Li_2ZnCl_4 (10 mL of 2 M in 0.1 M HCl) added, and the mixture cooled in ice for 5 min. The grey precipitate was filtered off, washed with oxygen-free acetone, and dried in vacuo; yield 0.84 g, 69%. Anal. Calcd for $CoC_{12}N_{14}H_{30}ZnCl_4 \cdot H_2O$: Co, 10.33; C, 25.25; N, 19.64; H, 5.65; Cl, 24.85. Found: Co, 10.5; C, 25.6; N, 19.2; H, 5.7; Cl, 25.3. The dithionate salt was synthesized similarly by reducing $[Co(sep)]Cl_3$ (0.5 g) in water (20 mL) with excess zinc dust. To the filtered solution were added a few drops of 1 M HCl followed by a solution of ~3 g $Li_2S_2O_6$ in deoxygenated water (2 mL). After 2 h at room temperature, the crystals were filtered off, washed with 96% ethanol, and dried in a vacuum desiccator. Anal. Calcd for $CoC_{12}N_8H_{30}S_2O_6 \cdot H_2O$: Co, 11.35; C, 27.75; N, 21.58; H, 5.42; S, 12.34. Found: Co, 11.6; C, 27.2; N, 21.1; H, 6.0; S, 13.0.

Synthesis of [(1,3,6,10,13,16,19-Heptaaza-8-methylbicyclo[6.6.6]eicosane)cobalt(III)] Trichloride-1.5-Water ([Co(azamesar)]Cl$_3$·1.5H$_2$O). To a stirred suspension of Li_2CO_3 (50 g) and (±)-$[Co(sen)]Cl_3$[3] (9.0 g, 0.022 mol) in water (90 mL) were added aqueous ammonia (240 mL of 2.1 M, 0.50 mol) and 36% aqueous formaldehyde (240 mL, 3.2 mol). The solutions were added separately and continuously over 2 h with a peristaltic pump. After another 15 min, the Li_2CO_3 was filtered off and the filtrate acidified with glacial acetic acid (50 mL) diluted with water (2 L) and sorbed on an ion-exchange column (Dowex 50W-X2, 200-400 mesh, H^+ form). The column was washed with 1 M HCl, and the complexes were removed with 3 M HCl. The eluate was taken down to dryness on a vacuum evaporator, and the solid compound was dissolved in water and sorbed on a Sephadex SP-C-25 ion-exchange column (36 × 15 cm). Two yellow bands separated on elution with 0.05 M trisodium citrate. The eluate containing the first and major band was then sorbed on a Dowex column, and after washing with 1 M HCl to remove Na^+ ions, the complex was taken off with 3 M HCl, taken down to dryness, and recrystallized by dissolving it in water (20 mL) and slowly adding acetone (200 mL); yield 6.1 g, 56%. Anal. Calcd for $CoC_{14}N_7H_{33}Cl_3 \cdot 1.5H_2O$: Co, 11.98; C, 34.19; N, 19.94; H, 7.38; Cl, 21.62. Found: Co, 11.8; C, 34.1; N, 20.5, H, 7.6; Cl, 21.9. Resolution of $[Co(azamesar)]^{3+}$ into its catoptric isomers Λ and Δ was achieved by ion-exchange chromatography. Pure racemic chloride (2.70 g) in water was adsorbed onto an ion-exchange column (Sephadex SP-C-25, Na^+

(1) Lehn, J. M. *Pure Appl. Chem.* **1977**, *49*, 857 and references therein.
(2) Creaser, I. I.; Harrowfield, J. MacB.; Herlt, A. J.; Sargeson, A. M.; Springborg, J.; Geue, R. J.; Snow, M. R. *J. Am. Chem. Soc.* **1977**, *99*, 3181.
(3) (a) Green, R. W.; Catchpole, K. W.; Philip, A. T.; Lions, F. *Inorg. Chem.* **1963**, *2*, 597. (b) Sarneski, J. E.; Urbach, F. L. *J. Am. Chem. Soc.* **1971**, *93*, 884 and references therein.

0002-7863/82/1504-6016$01.25/0

form, 10 × 25 cm). Elution with 0.02 M sodium antimony (+)-tartrate gave two bands of equal size. The complexes were isolated as the chloride salts by sorbing the tartrate eluates on a Dowex column (Na^+ form), washing thoroughly first with water and then with 1 M HCl, and eluting with 3 M HCl as before. The fastest moving isomer on the Sephadex column was the $(-)_{500}$-$\Lambda(S)$ isomer. Both isomers crystallized as [Co(azamesar)]$Cl_3 \cdot 1.5H_2O$. The synthesis of $[Co(azamesar)]^{3+}$ from $(+)_{589}$-[Co(sen)]Cl_3[3b] gave $(+)_{589}$-$[Co(azamesar)]^{3+}$.

[Co(*N*-Me(sen))]$Cl_3 \cdot 2H_2O$. The second band from the Sephadex ion-exchange chromatography in the $[Co(azamesar)]^{3+}$ synthesis was collected on Dowex and treated as above to give the chloride salt (0.75 g). The analysis indicated that the addition of 1 mol of CH_2O per mole of Co(III) had occurred. Anal. Calcd for $CoC_{12}N_6H_{32}Cl_3 \cdot 2H_2O$: Co, 12.77; C, 31.21; N, 18.21; H, 7.86; Cl, 23.03. Found: Co, 12.7; C, 31.6; N, 18.2; H, 7.5; Cl, 23.6.

Synthesis of [Co(azamesar)]$ZnCl_4 \cdot H_2O$. [Co(azamesar)]$Cl_3 \cdot 1.5H_2O$ (0.9 g) in water (40 mL) was reduced with a large excess of zinc dust under nitrogen. To the filtered solution (under nitrogen) was added HCl (0.5 mL of 1 M). After cooling, an ice-cold oxygen-free solution of Li_2ZnCl_4 (15 mL of 4 M) was added. The white precipitate was collected after 5 min, washed with a little ethanol (96%, N_2 saturated) and then ether (N_2 saturated) and dried in a desiccator under vacuum; yield 0.65 g, 61%. Anal. Calcd for $CoC_{14}N_7H_{33}ZnCl_4 \cdot H_2O$: Co, 10.10; C, 28.81; N, 16.80; H, 6.05; Cl, 24.30; Zn, 11.20. Found: Co, 10.3; C, 28.9; N, 16.6; H, 5.8; Cl, 24.1; Zn, 12.2.

Kinetic Experiments. All solutions were flushed with nitrogen for at least 3 h before each kinetic run and mixed in a stopped-flow apparatus that had been flushed with nitrogen as well. The electron-transfer reactions were studied by following the change in optical rotation of solutions containing $\Lambda(S)$-$[Co(sep)]^{2+}$ and $\Delta(R)$-$[Co(sep)]^{3+}$. Solutions of $\Lambda(S)$-$[Co(sep)]^{2+}$ in 0.2 M NaCl were made in situ by reducing solutions of $\Lambda(S)$-[Co(sep)]$Cl_3 \cdot H_2O$ with Zn powder or amalgamated Zn. The concentrations of the Co(II) solutions were determined either spectrophotometrically after complete oxidation by air to $[Co(sep)]^{3+}$ or were calculated from the concentration of the starting material. The $\Lambda(S)$-$[Co(sep)]^{2+}$ solution was mixed with a solution of $\Delta(R)$-$[Co(sep)]^{3+}$ in 0.2 M NaCl–HCl in a stopped-flow apparatus that was connected to a 5-cm polarimeter cell.

The kinetics of the oxidation of $[Co(sep)]^{2+}$ with O_2 were followed spectrophotometrically at 260 or 270 nm. Solutions of $[Co(sep)]^{2+}$ were prepared as above. Solutions of O_2 were made by mixing O_2-saturated water[4] with O_2-free aqueous NaCl–HCl solutions. The concentrations of $[Co(sep)]^{2+}$ in the reactant solutions were determined spectrophotometrically at 472 nm after complete oxidation to $[Co(sep)]^{3+}$ with excess O_2. Concentrations of H_2O_2 formed in the reaction solutions were determined iodometrically. In a separate experiment, the complex was sorbed on a short Dowex cation-exchange column after complete oxidation. The column was washed with water, and the combined eluates were tested for H_2O_2 iodometrically.

The reaction between $[Co(sep)]^{2+}$ and CF_3SO_3H was studied by following the change in absorption at 250 nm of a solution of $[Co(sep)]^{2+}$ mixed with solutions of CF_3SO_3H at constant ionic strength. Analogous experiments were also carried out with the $[Co(azamesar)]^{3+/2+}$ ions.

Isotope-Exchange Experiment. [Co(sep)]Cl_3 (0.451 g) was dissolved in H_2O (10 mL) and reduced with Zn dust under argon. ^{60}Co-labeled $CoCl_2$ solution (0.1 M, 10 mL, ~1000 counts/sec/mL) was deoxygenated with argon. Aliquots (1 mL) of the two solutions were mixed and stirred under argon for 17.5 h. The argon flow was discontinued and the passage of air used to oxidize the $[Co(sep)]^{2+}$ back to $[Co(sep)]^{3+}$. The oxidized solution was adsorbed onto a short cation-exchange column (Dowex 50W-X2, H^+ form, 5 × 1 cm) and the column washed with water. Co(II) was eluted with 0.5 M HCl (~100 mL) and $[Co(sep)]^{3+}$ with 3 M HCl. The eluates were reduced in volume and each finally made up to a volume of 10 mL. Count rates were then recorded from 1-mL aliquots of these solutions by using an EKCO (N550A NaI-Tl) well-type scintillation counter.

Results

Synthesis. The Co(III) complex of the macrobicycle 1,3,6,8,10,13,16,19-octaazabicyclo[6.6.6]eicosane ($[Co(sep)]^{3+}$) has been synthesized on the metal by condensing the $[Co(en)_3]^{3+}$ ion with formaldehyde and ammonia. Excesses of the reagents were added separately and simultaneously over ~2 h to a solution of $[Co(en)_3]^{3+}$ at pH ~10 to give the caged complex (74% calculated on the basis of $[Co(en)_3]^{3+}$). Besides the racemic form, both the $\Lambda(S)$ and $\Delta(R)$ forms of the complex were isolated when

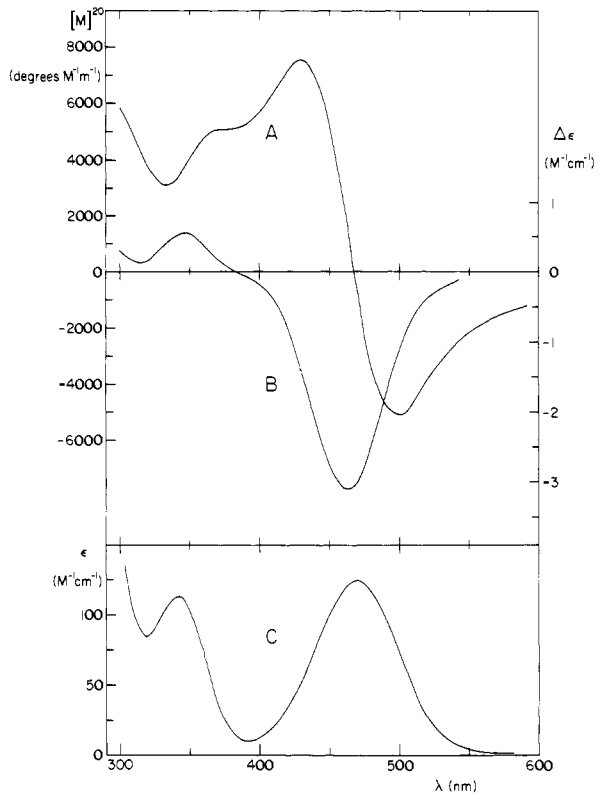

Figure 1. Rotary dispersion (A), circular dichroism (B), and visible absorption spectra (C) of Λ-[Co(azamesar)]$Cl_3 \cdot 1.5H_2O$ in H_2O.

Λ- and Δ-$[Co(en)_3]^{3+}$, respectively, were used. Attempts to resolve the racemic complex by precipitating it as the (+)-tartrate chloride salt were only partly successful.

With Zn powder or amalgamated Zn, reduction to $[Co(sep)]^{2+}$ took place quantitatively in aqueous solution for the conditions $10^{-7} \leq [H^+] \leq 10^{-2}$, and the Co(II) complex was isolated as the $ZnCl_4^{2-}$ or $S_2O_6^{2-}$ salt. When completely dry, the crystals had a nondescript grey color and were stable for days in air at room temperature. Reduction of chiral $[Co(sep)]^{3+}$ gave chiral $[Co(sep)]^{2+}$, which was stable to racemization in neutral or slightly acid aqueous solution for at least 2 h at 20 °C. Neutral solutions of racemic $[Co(sep)]^{2+}$ were stable for at least 3 days when kept over amalgamated Zn in an N_2 atmosphere.

The related cage complex $[Co(azamesar)]^{3+}$ was synthesized in essentially the same way as $[Co(sep)]^{3+}$, starting with the partially caged $[Co(sen)]^{3+}$ ion.[3] Its properties and reactions are closely related to those of $[Co(sep)]^{3+}$.

Spectra. Figures 2 and 3 of ref 2 show the visible absorption, rotary dispersion, and circular dichroism spectra of Λ-$[Co(sep)]^{3+}$ and Λ-$[Co(sep)]^{2+}$ ions. In H_2O, the molar absorptivies for the Co(III) complex at the maxima were $\epsilon_{472} = 109$ and $\epsilon_{340} = 116$ compared with those for the Co(II) complex ion $\epsilon_{910} = 4.94$, $\epsilon_{664} = 0.77$, $\epsilon_{552} = 1.76$, $\epsilon_{545} = 1.97$, $\epsilon_{539} = 1.87$, and $\epsilon_{467} = 8.21$. The molecular rotations in H_2O for the Co(III) complex were $[M]_{490} = -3790°$, $[M]_{428} = +6540°$, and $[M]_{378} = +5880°$, and the corresponding values for the Co(II) complex were $[M]_{556} = -350°$, $[M]_{543} = +100°$, $[M]_{530} = -120°$, $[M]_{517} = -192°$, and $[M]_{430} = +1800°$. The CD spectrum for the Λ-$[Co(sep)]^{3+}$ ion showed the following maxima in H_2O: $\Delta\epsilon_{461} = -2.37$, $\Delta\epsilon_{352} = +0.983$. The corresponding maxima for Λ-$[Co(sep)]^{2+}$ were $\Delta\epsilon_{675} = -0.015$, $\Delta\epsilon_{632} = -0.024$, $\Delta\epsilon_{545} = -0.249$, $\Delta\epsilon_{526} = -0.205$, $\Delta\epsilon_{490} = -0.482$, and $\Delta\epsilon_{450} = -0.258$. The corresponding spectra in H_2O of Λ-$[Co(azamesar)]^{3+}$ and Λ-$[Co(azamesar)]^{2+}$ are depicted in Figures 1 and 2. The molar absorptivities were $\epsilon_{469} = 125$ and $\epsilon_{342} = 114$ for $[Co(azamesar)]^{3+}$ and $\epsilon_{921} = 5.50$, $\epsilon_{644} = 0.93$, $\epsilon_{551} = 3.49$, $\epsilon_{515} = 4.56$, and $\epsilon_{463} = 8.63$ for $[Co(azamesar)]^{2+}$. The molecular rotations were $[M]_{500} = -5120°$, $[M]_{430} = +7540°$, and $[M]_{370} = 5100°$ for the Co(III) complex and $[M]_{626} = -1010°$, $[M]_{580} = -1280°$, $[M]_{529} = -470°$, $[M]_{470} = +1450°$, and $[M]_{437} =$

(4) Linke, W. F. "Solubilities, Inorganic and Metal-Organic Compounds", 4th ed.; American Chemical Society: Washington, D. C., 1965.

Table I. ^{13}C NMR Spectra (Ppm Relative to 1,4-Dioxane)

compound	NCH_2CH_2N	NCH_2N	NCH_2C	$C-CH_3$	tert C	$N-CH_3$
$[Co(en)_3]^{3+}$	−21.817					
$[Co(sen)]^{3+}$	−12.335		−9.869	−47.009	not obsd	
	−24.023					
$[Co(sep)]^{3+}$	−13.245	+0.389				
[Co(azamesar]$^{3+}$	−12.726	+0.519	−11.167	−47.139	−24.154	
	−14.024					
$[Co(Me-(sen))]^{3+}$	−12.726, −11.687					
	−12.336, −10.777					−28.049
	−23.375			−47.009	not obsd	−28.958
	−24.413					

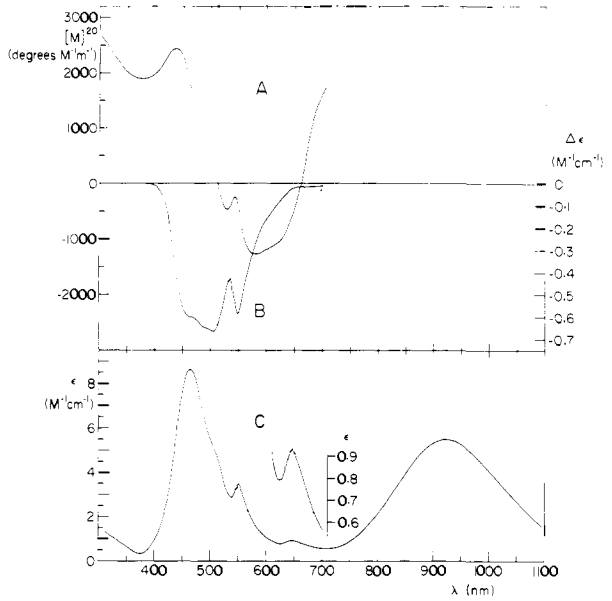

Figure 2. Rotary dispersion (A), circular dichroism (B), and visible absorption spectra (C) in H_2O of Λ-$[Co(azamesar)]^{2+}$ obtained by reducing Λ-$[Co(azamesar)]Cl_3 \cdot 1.5H_2O$ in water with Zn.

+2430° for the Co(II) complex. The CD spectrum for the Λ-$[Co(azamesar)]^{3+}$ ion gave the following maxima in H_2O, $\Delta\epsilon_{463} = -3.10$ and $\Delta\epsilon_{346} = +0.561$ and for the $[Co(azamesar)]^{2+}$ ion, $\Delta\epsilon_{549} = -0.585$, $\Delta\epsilon_{505} = -0.665$, $\Delta\epsilon_{491} = -0.653$, and $\Delta\epsilon_{463} = -0.602$. The spectral properties of the Co(II) and Co(III) complexes showed little dependence on $[H^+]$ in the region $10^{-7} \leq [H^+] \leq 10^{-2}$ and $10^{-7} \leq [H^+] \leq 1$, respectively.

Figure 3 gives the ^1H and ^{13}C NMR spectra in D_2O of N-deuterated $[Co(sep)]^{3+}$. In the proton spectrum, an AB doublet pair appears with $J \sim 12$ Hz at 4.0 ppm corresponding to 12 protons, which are ascribed to the methylene groups of the caps. A complex AA'BB' pattern occurs at ~3.2 ppm, also integrating for 12 protons and ascribed to the ethylenediamine methylene protons. The ^{13}C spectrum also shows a high degree of symmetry with just two signals of equal intensity at +0.389 and −13.245 ppm relative to 1,4-dioxane. The former signal is ascribed to the C atoms in the caps and the latter to the ethylenediamine skeleton.

The ^1H NMR spectrum of $[Co(azamesar)]^{3+}$ in D_2O showed very little sensitivity to change in pH. The spectra recorded in 3 M DCl after deuteration of the secondary amine groups in D_2O (pH ~7) and in Na_2CO_3–$NaDCO_3$–D_2O buffer (pH ~10.5) were surprisingly similar. The spectrum showed one singlet at 1.0 ppm, a complex pattern roughly described as one AB quartet superposed on another AB quartet (2.3–3.5 ppm) and, clearly separated, a typical AB quartet (3.7–4.4 ppm). Integration showed the ratio 3:18:6. Accordingly, the signals were interpreted as being due to the 3 methyl protons, the 18 methylene protons for the $N-C-H_2-CH_2-N$ and $N-CH_2-C$ groups, and 6 methylene protons of the nitrogen cap, $N-CH_2-N$. When strong base was added to a solution of $[Co(azamesar)]^{3+}$, the color instantly changed from yellow to red, but this color disappeared within seconds at room temperature to give a brown-yellow solution. The ^1H NMR

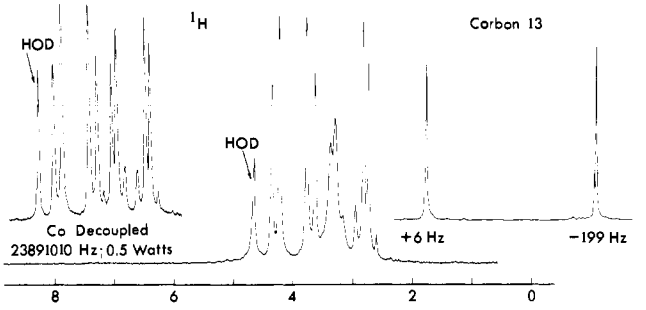

Figure 3. ^1H and ^{13}C NMR spectra of N-deuterated $[Co(sep)]Cl_3 \cdot H_2O$ in D_2O.

spectrum of this solution ([NaOD] = 0.1 M) was very similar to the spectrum in D_2O and did not show any change over 40 min at room temperature. Subsequent addition of excess DCl gave a solution that had an ^1H NMR spectrum identical with that of $[Co(azamesar)]^{3+}$. Conceivably, a very small amount of the complex ion could have reacted to give a new product, but so far this has not been detected. The ^{13}C NMR spectra and assignments of the azamesar and related complexes are given in Table I.

The magnetic moment of the $[Co(sep)]ZnCl_4$ salt was determined as $\mu_{eff} = 4.72\ \mu_B$ at 23 °C and of $[Co(azamesar)]ZnCl_4$ as $\mu_{eff} = 4.56\ \mu_B$ at 21 °C.

Redox Properties. Cyclic voltammetry studies using a Pt electrode gave an essentially reversible wave in 0.1 M $NaClO_4$ with $E_{1/2} = -0.54$ V vs. SCE or $E° = -0.30$ V for $[Co(sep)]^{3+/2+}$ and $E_{1/2} = -0.60$ V vs. SCE or $E° = -0.36$ V for $[Co(azamesar)]^{3+/2+}$ at a scan rate of 200 mV/s. The peak difference was 70 mV, and $i_{pc}/i_{pa} = 1.0$. Under the same condition, the reduction potential for $[Co(en)_3]^{2+/3+}$ was found to be $E_{1/2} = \sim -0.45$ V vs. SCE and irreversible. When the potentials were measured polarographically by using a dropping mercury electrode or by cyclic voltammetry using the mercury hanging drop (200 mV/s), reversibility was established for all three complexes giving $E°$ as −0.26 V for $[Co(sep)]^{3+/2+}$, −0.34 V for $[Co(azamesar)]^{3+/2+}$, and −0.13 V for $[Co(en)_3]^{3+/2+}$ in 0.1 M $NaClO_4$. The difference in results from the Pt and Hg electrodes was ascribed to the difficulty in obtaining clean Pt electrodes, and additional data[5] lead us to accept the Hg data as the more accurate values.

An aqueous solution equimolar (0.05 M) in $[Co(sep)]^{2+}$ and ^{60}Co-labeled Co^{2+} was kept under argon at 25 °C for 17.5 h. The $[Co(sep)]^{2+}$ was then oxidized to $[Co(sep)]^{3+}$ quantitatively with air and separated from Co_{aq}^{2+} by ion-exchange chromatography. Reduction of the eluates to the same volume gave the following count rates: Co_{aq}^{2+} 33 668 counts/min, $[Co(sep)]^{3+}$ 513 counts/min, and 5558 counts/10 min, background 5330 counts/10 min. Clearly, no significant incorporation of ^{60}Co into the cage was detected. The difference between background and $[Co(sep)]^{3+}$ counts is not significant at the 99% confidence level, and in any case, the counts above background for $[Co(sep)]^{3+}$ would indicate <0.1% exchange.

The Co(II) complex was oxidized by O_2 in aqueous solution to $[Co(sep)]^{3+}$ and H_2O_2 with more than 99% retention of the

(5) Lay, P. A. Ph.D. Thesis, Australian National University, 1981.

Table II. Rate Constants for the Oxidation of $[Co(sep)]^{2+}$ with O_2 at 25 °C, μ = 0.2 (NaCl), 260 and 270 nm

$[O_2]^a \times 10^5$ M	$[Co]^a \times 10^5$ M	$[H^+]$, M	$k_{obsd} \times 10^2$ s^{-1}	k,[b] M^{-1} s^{-1}
52.7	3.7	0.001	4.13	39.2
52.7	3.7	0.01	4.17	39.6
52.7	3.7	0.10	4.55	43.2
25 9	3.7	0.001	2.10	40.5
52.7	3.7	0.001	4.31	40.8
2.98	86.9	0.001	4 26	49.0
2.98	39.4	0.001	1 79	45.4

[a] For the reactant A in excess, the concentration is given as $[A]_{av} = ([A]_{t_0} - [A]_{t_\infty})/2$. [b] $k = k_{obsd}/2[O_2]_{av}$ or $k = k_{obsd}/[Co]_{av}$.

Table III Stoichiometry Data for the Oxidation of $[Co(sep)]^{2+}$ by O_2 in H_2O ($[O_2] = 1.3 \times 10^{-3}$ M)

$[Co] \times 10^4$ M	$[H_2O_2] \times 10^4$ M	% theoretical yield
1.74	0.91	105
2.33	1.11	95
4.57	2.25	98
7.30	3.52	96

absolute configuration for $10^{-7} < [H^+] < 10^{-2}$. $\epsilon_{472} = 108$ in H_2O and $[M]_{492} = -3630°$ in 0.01 M HCl for reoxidized Λ-$[Co(sep)]^{2+}$ compared to $\epsilon_{472} = 109$ and $[M]_{492} = -3610°$ for authentic Λ-$[Co(sep)]^{3+}$. The results are given in Table II. For pseudo-first-order conditions with excess O_2 or Co(II), a rate law of the form $-d[O_2]/dt = -^1/_2 d[Co(sep)^{2+}]/dt = k_{ox}[Co(sep)^{2+}][O_2]$ was obtained with $k_{ox} = 43 \pm 5$ M^{-1} s^{-1}. The second-order rate constant was found to be independent of $[H^+]$ for $10^{-3} \leq [H^+] \leq 10^{-1}$.

The stoichiometry of the reaction is given by

$$2[Co(sep)]^{2+} + O_2 + 2H^+ \rightarrow 2[Co(sep)]^{3+} + H_2O_2 \quad (1)$$

The $[Co(sep)]^{3+}$ was identified by its visible spectrum and the H_2O_2 by its reaction with iodide ion to give iodine. The concentration of H_2O_2 in the completed reaction mixture was determined iodometrically (Table III) and was found to correspond to the concentration calculated according to eq 1. After the complex was removed from the reaction mixture by a cation-exchange column, about 90% H_2O_2 was detected. The reaction between $[Co(sep)]^{2+}$ and H_2O_2 was slower than that with O_2 ($\sim$10-fold), and it did not interfere with the oxidation by O_2. It was not studied in detail.

The kinetics of the electron-transfer reactions were studied by measuring the rate of racemization of solutions that initially contained the ions Λ-$[Co(sep)]^{2+}$ and Δ-$[Co(sep)]^{3+}$. Electron transfer between equal concentrations of Λ-Co(II) and Δ-Co(III) leads to racemization, and the rate can be followed readily by the change in rotatory power (α) at 490 nm.[6,7] The data (Table IV) obey a rate law of the form $-(d \ln (\alpha - \alpha_\infty))/dt = k_{et}[Co]_{total}$ where $k_{et} = 5.1 \pm 0.3$ M^{-1} s^{-1} at 25 °C and μ = 0.2. Plots of $\ln (\alpha - \alpha_\infty)$ vs. time were linear for $\sim$3 half-lives. From this constant and those measured at 15 and 40 °C, the following activation parameters were calculated: $\Delta H^\ddagger = 9.6 \pm 0.5$ kcal/mol, $\Delta S^\ddagger = -23 \pm 2$ cal/(deg mol). The analogous rate constant for the self-exchange reaction for $[Co(azamesar)]^{3+/2+}$ was found to be 2.9 M^{-1} s^{-1}.

The corresponding electron-transfer rate constant for $[Co(en)_3]^{2+/3+}$ at 25 °C and μ = 0.98 is 7.7×10^{-5} M^{-1} s^{-1} with $\Delta H^\ddagger$ = 13.6 kcal/mol and $\Delta S^\ddagger = -32$ cal/(deg mol) measured by the same method[7] or 5.2×10^{-5} M^{-1} s^{-1} and μ = 1 measured by the isotopic exchange method.[8] For $[Co(NH_3)_6]^{2+/3+}$, the self-exchange rate has recently been estimated as $k \gtrsim 10^{-7}$ M^{-1} s^{-1} at 25 °C.[9]

(6) Dwyer, F. P.; Gyarfas, E. C. *Nature* (London) **1950**, *166*, 481.
(7) Dwyer, F. P.; Sargeson, A. M. *J. Phys. Chem.* **1961**, *65*, 1892.
(8) Lewis, W. B.; Coryell, C. D.; Irvine, J. W. *J. Chem. Soc. Suppl. No. 2*, **1949**, 386.

Table IV. Rate Constants for the Electron Transfer of Caged Metal Ions

$\Lambda(S)$-$[Co(sep)]^{2+}$ + $\Delta(R)$-$[Co(sep)]^{3+}$, μ = 0.2 (NaCl), 490 nm

$[Co]_{total} \times 10^3$ M	$[Co(III)]_{t_0}/[Co(II)]_{t_0}$	T, °C	$k_{obsd} \times 10^2$ s^{-1}	k, M^{-1} s^{-1}
2.26	0.59	25	1.09[a]	4.82
2.60	0.71	25	1.24	4.78
2.80	0.19	25	1.43	5.09
2.90	4.3	25	1.63	5.61
1.10	2.5	25	0.55	5.01
1.24	0.47	25	0.675	5.44
4.97	0.13	25	2.53	5.10
1.92	1.65	25	0.95	4.87
2.13	1.43	25	1.03[b]	
1.92	1.65	15	0.50	2.6 ± 0.2
1.92	1.65	40	2.08	10.7 ± 0.4
2.09	0.84	25	2.57[c]	11.5

$\Lambda(S)$-$[Co(azamesar)]^{2+}$ + $\Delta(R)$-$[Co(azamesar)]^{3+}$, μ = 0.2 (NaCl), 500 nm

$[Co]_{total} \times 10^3$ M	$[Co(III)]_{t_0}/[Co(II)]_{t_0}$	T, °C	$k_{obsd} \times 10^2$ s^{-1}	k, M^{-1} s^{-1}
1.70	2.6	25	0.508	2.99
1.46	0.55	25	0.419	2.87

[a] 0.19 M NaCl, 0.01 M HCl. [b] 0.2 M $LiClO_4$. [c] 0.5 M NaCl.

Table V. Rate Constants for the Decomposition of $[Co(sep)]^{2+}$ in Acid Solution at 25 °C, μ = 1.0 ($LiCF_3SO_3$), 250 nm

$[Co(sep)]^{2+}$, M	$[CF_3SO_3H]$, M	$k_{obsd} \times 10^2$ s^{-1}	$k \times 10^2$ M^{-1} s^{-1}
10^{-3}	1.0	1.13 (6)[a]	1.13 ± 0.3
10^{-3}	0.75	0.89 (5)	1.2 ± 0.1
10^{-3}	0.50	0.60 (3)	1.2 ± 0.1
5×10^{-4}	0.30	0.396 (3)	1.3 ± 0.1
5×10^{-4}	0.10	0.124 (2)	1.2 ± 0.1

[a] Number of experiments is in parentheses.

When $[Co(sep)]^{3+}$ was reduced with Zn in acid solution or solutions of $[Co(sep)]^{2+}$ were acidified, decomposition of the cage to Co_{aq}^{2+}, $NH_3(CH_2)_2NH_3^{2+}$, and NH_4^+ took place. The rate of decomposition of $[Co(sep)]^{2+}$ was followed spectrophotometrically at 250 nm at 25 °C in CF_3SO_3H solutions with $1 \leq [H^+] \leq 0.1$ and μ = 1.0 (Table V). The rate law, $-d[Co(sep)^{2+}]/dt = k[Co(sep)^{2+}][H^+]$, yielded a second-order rate constant of 1.2×10^{-2} M^{-1} s^{-1}.

When the cage complexes were dissolved in strongly basic solution (pH $\geq$13), a color change from yellow to dark purple to yellow-brown occurred. Acidification restored the original yellow color. This behavior was attributed to deprotonation of one or more secondary amino groups in the basic solution. However, attempts to determine the pK_a by titration were unsuccessful but the inconclusive data indicated that it was in the interval 13–14 at 25 °C. The $[Co(sep)]^{3+}$ complex is capped by two tertiary noncoordinated nitrogen atoms that superficially might be expected to be strongly basic. However, solutions of the complex in water were neutral, and all attempts to protonate the tertiary nitrogen atoms were unsuccessful. $[Co(sep)]Cl_3$ is isolated unaltered from 12 M HCl, and we assert therefore that the pK_a of the protonated cap N atoms is less than zero in this ion.

X-ray Crystallographic Analysis of $(+)_{490}[Co(sep)]S_2O_6 \cdot H_2O$

Crystal Data. Preliminary precession photographs indicated space group $P2_12_12_1$. A crystal with dimensions 0.12 × 0.13 × 0.4 mm was smeared with epoxy resin to reduce aerial oxidation and mounted about the needle axis c. Unit cell dimensions were obtained from the axial reflections on a Stoe Weissenberg diffractometer by using graphite-monochromated Mo Kα radiation (λ 0.7107 Å) and are a = 15.67 (1) Å, b = 15.411 (6) Å, and c = 8.757 (4) Å. With Z = 4 and the formula weight of 523.5 for $CoC_{12}H_{30}N_8S_2O_6 \cdot H_2O$, the calculated density is 1.647 g cm^{-3}.

(9) Geselowitz, G.; Taube, H., to be published.

Table VI. Least-Squares Positional and Thermal Parameters of $(+)_{490}$-$[Co^{II}(sep)]S_2O_6 \cdot H_2O$[a]

atom	x	y	z	β_{11}	β_{22}	β_{33}	β_{12}	β_{13}	β_{23}
Co	14990 (7)	25343 (8)	24567 (14)	175 (4)	170 (4)	492 (13)	0 (5)	10 (7)	4 (9)
S(1)	43128 (16)	37899 (17)	21562 (31)	243 (10)	317 (11)	830 (39)	−46 (9)	−11 (16)	22 (16)
S(2)	55249 (14)	44173 (16)	21001 (28)	196 (9)	284 (11)	655 (34)	−2 (8)	−9 (14)	−62 (15)
O(W)	5155 (7)	1709 (6)	3380 (14)	85 (7)	43 (5)	291 (25)	6 (5)	−94 (11)	10 (9)
O(1)	4432 (6)	3027 (4)	1224 (12)	62 (5)	58 (5)	188 (17)	−21 (5)	20 (8)	−53 (8)
O(2)	4196 (6)	3568 (6)	3736 (11)	46 (5)	74 (6)	134 (16)	−19 (4)	6 (7)	28 (8)
O(3)	3695 (5)	4402 (6)	1588 (13)	26 (3)	54 (5)	322 (23)	0 (3)	−29 (7)	53 (9)
O(4)	6098 (4)	3767 (5)	2740 (11)	31 (3)	44 (4)	154 (15)	13 (3)	−12 (6)	5 (7)
O(5)	5421 (5)	5188 (4)	3045 (9)	36 (4)	32 (3)	113 (13)	−2 (3)	−4 (6)	−17 (5)
O(6)	5671 (5)	4599 (5)	519 (9)	30 (3)	43 (4)	87 (12)	−5 (3)	9 (5)	4 (6)
N(1)	2001 (5)	1633 (5)	805 (11)	18 (3)	29 (4)	74 (14)	3 (3)	3 (6)	−6 (6)
N(2)	2594 (5)	2302 (5)	3912 (10)	20 (3)	26 (4)	73 (13)	3 (3)	−5 (5)	−1 (5)
N(3)	862 (5)	1478 (5)	3611 (10)	24 (4)	18 (4)	78 (13)	1 (3)	−2 (6)	3 (5)
N(4)	1998 (6)	3472 (5)	816 (12)	25 (2)	27 (4)	80 (15)	−5 (3)	−3 (6)	13 (6)
N(5)	1297 (5)	3579 (5)	4044 (10)	28 (4)	22 (4)	75 (13)	3 (3)	2 (5)	−5 (6)
N(6)	226 (5)	2764 (5)	1571 (10)	25 (4)	24 (4)	76 (13)	1 (3)	14 (5)	8 (5)
N(7)	2263 (6)	780 (6)	3160 (11)	34 (4)	24 (4)	114 (16)	6 (4)	2 (6)	2 (6)
N(8)	721 (6)	4278 (5)	1731 (11)	45 (4)	16 (4)	99 (14)	7 (3)	−7 (6)	9 (5)
C(1)	2433 (8)	876 (7)	1577 (15)	34 (5)	29 (5)	119 (21)	11 (4)	4 (8)	−12 (8)
C(2)	2736 (8)	1330 (8)	4216 (15)	37 (5)	35 (6)	116 (19)	14 (5)	−15 (8)	8 (8)
C(3)	1372 (7)	650 (6)	3527 (15)	32 (5)	21 (4)	154 (20)	1 (4)	6 (8)	14 (8)
C(4)	2561 (7)	2124 (7)	−268 (14)	31 (5)	37 (5)	81 (18)	−2 (4)	19 (7)	7 (7)
C(5)	2445 (7)	2801 (7)	5342 (13)	28 (5)	41 (6)	75 (17)	0 (4)	−10 (7)	−1 (7)
C(6)	−1 (6)	1378 (6)	2873 (13)	23 (4)	29 (5)	113 (20)	−7 (3)	6 (7)	3 (8)
C(7)	2140 (7)	2979 (8)	−615 (13)	29 (5)	45 (6)	69 (17)	−7 (5)	7 (7)	9 (8)
C(8)	−351 (5)	2293 (6)	2615 (13)	21 (3)	36 (5)	86 (15)	1 (3)	3 (7)	4 (8)
C(9)	2108 (7)	3696 (6)	4905 (13)	32 (5)	22 (5)	81 (16)	1 (4)	−12 (7)	−13 (7)
C(10)	23 (7)	3709 (8)	1416 (15)	28 (5)	35 (5)	147 (20)	11 (4)	−10 (8)	15 (9)
C(11)	1410 (9)	4248 (7)	633 (15)	55 (7)	23 (5)	131 (20)	−1 (5)	14 (10)	20 (8)
C(12)	961 (9)	4394 (7)	3307 (14)	61 (7)	24 (5)	110 (21)	12 (5)	−12 (9)	−2 (8)

[a] Co and S × 10^5, others × 10^4. The form of the anisotropic thermal ellipsoid is $\exp[-(\beta_{11}h^2 + \beta_{22}k^2 + \beta_{33}l^2 + 2\beta_{12}hk + 2\beta_{23}kl)]$.

The density measured by flotation is 1.66 g cm^{-3}.

Intensity Data Collection. The above crystal was mounted about the *c* axis, and diffraction data were collected for the layers *hk*0–*hk*9 by the ω scan method to $2\theta = 55°$. The scan range was 1° on the zero layer and incremented for the upper levels according to $\Delta\omega = 1.0 + 0.6(\sin u/\tan(\psi/2))$ where u is the equiinclination angle and ψ is the detector angle. A standard reflection monitored after every 30 reflections and a zero layer collected at the end of the run indicated no significant crystal decomposition. A total of 1895 reflections with $I > 3\sigma(I)$ were measured and corrected for Lorentz and polarization effects but not for absorption as the transmission factors varied by less than 1%.

Structure Solution and Refinement.[10] The structure was solved by the heavy-atom method and refined by full-matrix least squares. Since the reflections were measured under approximately constant-count conditions, unit weights were adopted throughout, and all non-hydrogen atoms were treated anisotropically. All hydrogens were included at their calculated positions (N–H = 0.91 Å, C–H = 0.99 Å)[11] except for the water hydrogens, which could not be located or calculated unambiguously. The single-axis layers of data were individually scaled during the isotropic refinement stage to give the correct relative scaling. Final cycles of anisotropic refinement were done in blocks alternating the overall scale factor and non-hydrogen coordinates in one cycle with the scale factor and thermal parameters in the next. This reduced R to 0.043, where $R = \sum||F_o| - |F_c||/\sum|F_o|$, and the final estimated error in an observation of unit weight was 1.5 e. A final difference-Fourier map showed no peak heights larger than 0.6 e/Å^3. The absolute configuration was verified by reversing the signs of $\Delta f''$ for Co and S and repeating the final cycles of least-squares refinement. R converged to 0.048, which virtually excludes this configuration on the basis of Hamilton's statistical criteria.[12]

Table VII. Calculated Hydrogen Atom Positions[a] (×10^4)

atom	x	y	z
C(1)H(1)	2251	338	1014
C(1)H(2)	3077	974	1432
C(2)H(1)	3367	1183	4130
C(2)H(2)	2530	1190	5303
C(3)H(1)	1114	256	2698
C(3)H(2)	1331	334	4554
C(4)H(1)	2637	1762	−1239
C(4)H(2)	3140	2221	229
C(5)H(1)	3004	2844	5956
C(5)H(2)	2006	2475	6000
C(6)H(1)	62	1063	1861
C(6)H(2)	391	1024	3581
C(7)H(1)	2521	3332	−1354
C(7)H(2)	1563	2877	−1160
C(8)H(1)	−953	2267	2213
C(8)H(2)	−364	2620	3668
C(9)H(1)	2550	4011	4242
C(10)H(1)	−197	3817	328
C(10)H(2)	−471	3844	2164
C(11)H(1)	1158	4230	−444
C(11)H(2)	1768	4800	746
C(12)H(1)	1449	4854	3346
C(12)H(2)	460	4628	3911
N(1)H(1)	1556	1414	274
N(2)H(1)	3076	2523	3440
N(3)H(1)	782	1621	4608
N(4)H(1)	2517	3669	1149
N(5)H(1)	888	3404	4757
N(6)H(1)	180	2502	626
C(9)H(2)	2017	4062	5884

[a] Isotropic temperature factors for C(*i*)H(*j*) were 4.0 and for N(*i*)H(1) 3.0 Å^2.

Co^+ scattering factors were used for Co(II), and these with the neutral atom curves for all other species were taken from Cromer and Waber's compilation.[13] Values of $\Delta f'$ and $\Delta f''$ for Co and Cl were acquired from the Tables of Cromer and Liberman.[14]

(10) In addition to local programs for the University of Adelaide's Cyber 173, the following programs or modifications were used: Zalkin's FORDAP Fourier program; FUORFLS, a modification by Taylor of Busing, Martin, and Levy's ORFLS program; ORFEE, a function and error program by Busing, Martin, and Levy; Blount's geometry program BLANDA; Johnson's ORTEP, a thermal ellipsoid-plot program.

(11) Geue, R. J.; Snow, M. R. *Inorg. Chem.* **1977**, *16*, 231.

(12) Hamilton, W. C. *Acta Cyrstallogr.* **1965**, *18*, 502.

(13) "International Tables for X-ray Crystallography"; Kynoch Press: Birmingham, England, 1974; Vol. IV, p 72.

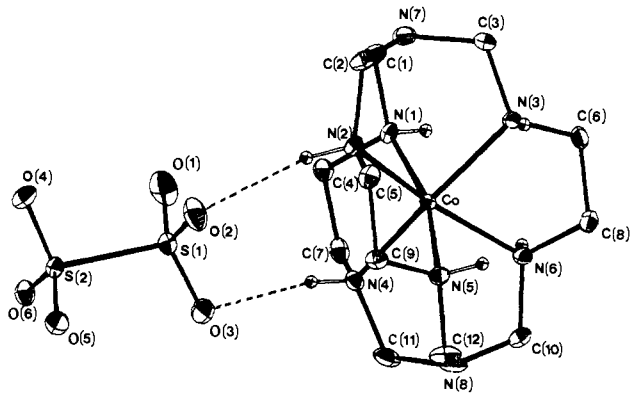

Figure 4. ORTEP diagram of $[Co(sep)]S_2O_6 \cdot H_2O$ with 20% thermal ellipsoids.

Table VIII. Interatomic Distances[a] (Å) for $[Co^{II}(sep)]S_2O_6 \cdot H_2O$

Co-N(1)	2.154 (9)	C(8)-N(6)	1.478 (12)
Co-N(2)	2.167 (8)	C(9)-N(5)	1.490 (13)
Co-N(3)	2.160 (8)	C(en)-N(lig) (av)	1.490
Co-N(4)	2.183 (9)	C(4)-C(7)	1.504 (16)
Co-N(5)	2.150 (8)	C(5)-C(9)	1.526 (15)
Co-N(6)	2.169 (8)	C(6)-C(8)	1.530 (14)
Co-N (av)	2.164	C-C (av)	1.520
C(1)-N(7)	1.419 (15)	S(1)-O(1)	1.443 (9)
C(2)-N(7)	1.457 (15)	S(1)-O(2)	1.437 (10)
C(3)-N(7)	1.447 (14)	S(1)-O(3)	1.440 (8)
C(10)-N(8)	1.428 (14)	S(2)-O(4)	1.458 (7)
C(11)-N(8)	1.447 (15)	S(2)-O(5)	1.456 (7)
C(12)-N(8)	1.442 (15)	S(2)-O(6)	1.431 (8)
C-N(cap) (av)	1.440	S-O (av)	1.444
C(1)-N(1)	1.509 (15)	S(1)-S(2)	2.132 (3)
C(2)-N(2)	1.539 (14)	O(2)···N(2)	3.182 (12)
C(3)-N(3)	1.508 (13)	O(3)···N(4)	3.095 (12)
C(10)-N(6)	1.498 (13)	O(1)···O(w)	2.996 (15)
C(11)-N(4)	1.518 (14)	O(2)···O(w)	3.250 (14)
C(12)-N(5)	1.508 (14)	O(4)···O(w)	3.544 (12)
C(cap)-N(lig) (av)	1.513	O(1)···N(6^{i})	3.004 (13)
C(4)-N(1)	1.493 (14)	O(4)···N(3^{i})	3.467 (13)
C(5)-N(2)	1.487 (14)	O(6)···N(1^{i})	3.048 (11)
C(6)-N(3)	1.507 (13)	N(1)···O(4^{ii})	3.467 (13)
C(7)-N(4)	1.483 (15)		

[a] Symmetry transformations: i, $^1/_2 + x$, $^1/_2 - y$, $-z$; ii, $-^1/_2 + x$, $^1/_2 - y$, $-z$.

Structure factors (electrons × 10) and root-mean-square vibration amplitudes of non-hydrogen atoms along the principal thermal ellipsoid axes are available. Tables VI and VII contain the final atomic parameters.

Description of the Structure. Figure 4 shows the $[Co(sep)]^{2+}$ cation hydrogen bonded to the dithionate anion. Table VIII contains the interatomic distances, and the cationic bond and torsion angles are given in Tables IX and X. The crystal cations and anions are linked through a two-dimensional hydrogen-bonding network with N(3)(H), N(5)(H), and O(5) excluded from the scheme. The water molecule is hydrogen bonded to oxygens O(1) and O(2) at one end of the dithionate ion, with a longer contact to O(4) at the other end. The dithionate ion also forms pairs of contacts with the protons of nitrogens N(2), N(4) (Figure 4) and N(1), N(6). These O···N distances lie within the range 3.004 (13) to 3.182 (12) Å and satisfy the empirical geometric criteria for significant hydrogen bonding. Another contact to N(3) of 3.467 (13) Å is trans to the N(3)H proton and therefore nonhydrogen bonding.

The Co(II)-N bond lengths average 2.164 Å, and individual values span a range of 0.033 Å. This variation is barely significant when the standard deviation of 0.009 Å in the individual distances is considered. The most plausible explanation for the relative differences is based on the variation in hydrogen-bond strength between corresponding NH groups and the dithionate anion in the crystal lattice. The three longest bonds Co-N(2) (2.167 (8) Å), Co-N(4) (2.183 (9) Å), and Co-N(6) (2.169 (8) Å) have associated N-H···O contacts that satisfy the geometric criteria for hydrogen bonding (N···O varies from 3.004 (13) to 3.182 (12) Å). The shorter bonds Co-N(5) (2.150 (8) Å) and Co-N(3) (2.160 (8) Å) have no close N-H···O contacts, although there is an electrostatic N···O contact with N(3) (O(4)···N(3^{i}) is 3.467 (13) Å) that is roughly perpendicular to Co-N(3) and could account for its slightly longer value. The other short bond, Co-N(1) (2.154 (9) Å) is hydrogen bonded to O(6) (N(1^{i})···O(6) is 3.048 (11) Å), and this appears to contradict the correlation between Co-N distance and hydrogen-bond strength. But there is also a repulsive electrostatic contact between N(1) and O(4^{ii}) (N(1)···O(4^{ii}) is 3.467 (13) Å) with a force component in the direction N(1) → Co along the bond axis. This contact would induce a compression of the Co-N(1) bond in opposition to the hydrogen-bonding forces. The observed variance in Co-N distance is then explained in terms of hydrogen bonding and coulombic lattice forces. Since the complex is shown to be high spin with the $(t_{2g})^5(e_g)^2$ octahedral electronic configuration, a very small Jahn-Teller elongation along one of the pseudotetragonal axes is expected. However, because of the low degree of ligand interaction with the t_{2g} orbitals in this type of complex, the distortion may not be significant at the present level of structural accuracy and may well be trivial compared with those effects arising from ligand constraints and lattice forces.

The average Co(II)-N distance of 2.155 (6) Å found here for the non-hydrogen-bonded nitrogens may be compared with the recently refined[15] value of 2.16 ± 0.005 Å found in the cubic

Table IX. Bond Angles (Deg) for $[Co^{II}(sep)]S_2O_6 \cdot H_2O$

C(1)-N(7)-C(3)	114.4 (1.0)	N(3)-C(6)-C(8)	106.9 (0.7)
C(1)-N(7)-C(2)	117.7 (1.0)	N(4)-C(7)-C(4)	110.1 (0.9)
C(2)-N(7)-C(3)	115.5 (1.0)	N(5)-C(9)-C(5)	108.1 (0.8)
C(10)-N(8)-C(12)	117.5 (1.0)	N(6)-C(8)-C(6)	108.9 (0.8)
C(11)-N(8)-C(12)	116.5 (1.0)	N(1)-Co-N(4)	81.6 (0.3)
C(10)-N(8)-C(11)	115.0 (1.0)	N(2)-Co-N(5)	81.9 (0.3)
N(7)-C(1)-N(1)	115.7 (1.0)	N(3)-Co-N(6)	82.3 (0.3)
N(7)-C(2)-N(2)	112.5 (0.9)	N(1)-Co-N(2)	89.9 (0.3)
N(7)-C(3)-N(3)	113.8 (0.8)	N(2)-Co-N(3)	88.1 (0.3)
N(8)-C(12)-N(5)	113.4 (1.0)	N(3)-Co-N(1)	89.8 (0.3)
N(8)-C(11)-N(4)	114.1 (0.9)	N(4)-Co-N(5)	89.0 (0.3)
N(8)-C(10)-N(6)	114.7 (0.8)	N(4)-Co-N(6)	89.2 (0.3)
C(1)-N(1)-C(4)	114.3 (0.8)	N(5)-Co-N(6)	88.5 (0.3)
C(2)-N(2)-C(5)	112.4 (0.9)	Co-N(1)-C(1)	111.2 (0.7)
C(3)-N(3)-C(6)	111.5 (0.8)	Co-N(2)-C(2)	112.1 (0.6)
C(7)-N(4)-C(11)	113.9 (0.9)	Co-N(3)-C(3)	111.8 (0.6)
C(8)-N(6)-C(10)	113.8 (0.8)	Co-N(5)-C(12)	113.5 (0.7)
C(9)-N(5)-C(12)	114.4 (0.8)	Co-N(4)-C(11)	111.9 (0.7)
N(1)-C(4)-C(7)	108.3 (0.8)	Co-N(6)-C(10)	112.7 (0.6)
N(2)-C(5)-C(9)	108.1 (0.9)		

Table X. Bond Torsion Angles[a] (Deg) for $[Co^{II}(sep)]S_2O_6 \cdot H_2O$

I J K L	
N(7)-C(1)-N(1)-C(4)	+136.9 (1.1)
N(7)-C(2)-N(2)-C(5)	+135.4 (0.9)
N(7)-C(3)-N(3)-C(6)	+138.5 (1.0)
N(8)-C(11)-N(4)-C(7)	+128.9 (1.0)
N(8)-C(12)-N(5)-C(9)	+131.9 (1.0)
N(8)-C(10)-N(6)-C(8)	+125.5 (1.0)
C(1)-N(1)-C(4)-C(7)	+164.9 (0.9)
C(2)-N(2)-C(5)-C(9)	+166.9 (0.9)
C(3)-N(3)-C(6)-C(8)	+164.3 (0.9)
C(10)-N(6)-C(8)-C(6)	+171.3 (0.8)
C(11)-N(4)-C(7)-C(4)	+167.4 (0.8)
C(12)-N(5)-C(9)-C(5)	+170.3 (0.9)
N(1)-C(4)-C(7)-N(4)	+58.4 (1.1)
N(2)-C(5)-C(9)-N(5)	+60.1 (1.1)
N(3)-C(6)-C(8)-N(6)	+61.7 (1.0)

[a] The torsion angle about the J-K bond is the angle the K-L bond is rotated from the IJK plane. It is positive when from IJ to KL the rotation is clockwise.

(14) Cromer, D. T.; Liberman, D. *J. Chem. Phys.* **1970**, *53*, 1891.

(15) Freeman, H. C., to be published.

Scheme I

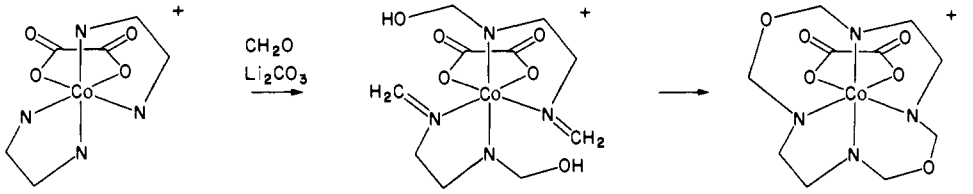

(F_{m^3m}) structure of $[Co^{II}(NH_3)_6]Cl_2$,[16] in which the Co(II) site has O_h symmetry and the NH_3 groups are not strongly hydrogen bonded. This indicates that the Co(II)–N bonds in $[Co(sep)]S_2O_6 \cdot H_2O$ may be slightly compressed by the ligand cage although the difference is barely significant at the present level of accuracy.

The C–N bonds alternate in length along the chain from the cap nitrogen, N(cap), to the first carbon of the ethylene bridge, C(en). The distances averaged over D_3 equivalents are given in Table VIII and vary sequentially from 1.440 (6) to 1.513 (6) to 1.490 (6) Å in the chain N(cap)–C(cap)–N(ligator)–C(en). A similarly averaged variation of 1.443 (8) to 1.523 (7) to 1.493 (9) Å was found in the $(-)_{490}$-$[Co^{III}(sep)]Cl_3 \cdot H_2O$ structure.[2] Each of the individual chains in both of these structures shows an equivalent C–N bond-length variance. The average C(cap)–N(cap)–C(cap) angle in $[Co^{II}(sep)]S_2O_6 \cdot H_2O$ is 116.1 (4)° compared with a value of 113.9 (4)° found in $(-)_{490}$-$[Co^{III}(sep)]Cl_3 \cdot H_2O$.[2] In the recently determined structure of hexamethylenetetramine thiourea,[17] the N(cap)–C(cap) distance of 1.474 (2) Å is normal for a C–N bond of this type[18] and about 0.03 Å longer than the values of 1.440 (6) and 1.443 (8) Å in the $[Co(sep)]^{2+/3+}$ structures. The C(cap)–N(cap)–C(cap) angle in hexamethylenetetramine is closely tetrahedral (108°) and 6–8° lower than the corresponding angles in the flattened caps of $[Co^{III}(sep)]^{3+}$ and $[Co^{II}(sep)]^{2+}$. The most apparent conclusion is that the C(cap)–N(cap) bond shortening is directly related to the C(cap)–N(cap)–C(cap) angle opening (or cap flattening). The mechanism for this coupling is consistent with an approach by the N(cap) valence orbitals toward sp^2 hybridization as the C(cap)–N(cap)–C(cap) angles expand. The nonhybridized $2p_z$ orbital of N(cap) then has the right symmetry for favorable (bonding) interaction with three antibonding components of three $-CH_2-$ molecular orbitals in a cap. This of course would effectively decrease the bond strengths of the adjoining N(ligator)–C(cap) bonds and imply an increase in their bond lengths. Indeed, an examination of Table VIII clearly shows that the N(ligator)–C(cap) distance is always greater than the N(ligator)–C(en) distance in the same N–C–N–C chain of the $[Co(sep)]S_2O_6 \cdot H_2O$ structure and this effect is also observed in the structure of $[Co^{III}(sep)]Cl_3 \cdot H_2O$.[2]

Further evidence for this modified bonding mechanism in the trigonal caps of the $[Co(sep)]^{2+/3+}$ ions comes from two sources. Detailed molecular mechanics calculations[19] by fast energy-minimization techniques on several conformations of $[Co(sep)]^{2+}$ and $[Co(sep)]^{3+}$ show that the observed distance and angular geometries found in the corresponding crystal structures are only reproduced accurately when the bond-stretching and angle-bending force constants for the C(cap)–N(cap)–C(cap) moieties are increased and those for C(cap)–N(ligator)–C(en) are reduced (except for the N(ligator)–C(en) stretch) relative to the normal saturated ones. This result is expected for increases in the C(cap)–N(cap) bond orders and decreases in the N(ligator)–C(cap) bond orders. Furthermore, it has been demonstrated that the N(cap) nitrogen is not protonated even in very concentrated hydrochloric acid ($pK_a < 0$). This is consistent with the argument proposed above for the bonding mechanism in the caps in which the N(cap) nitrogens would have reduced proton affinities.

The question as to whether the flattening of the trigonal caps induces the observed electronic and bond-order changes or whether the inverse occurs is a subtle one and may well depend on the overall stereochemistry of the compound. For the $[Co(sep)]S_2O_6 \cdot H_2O$ and $[Co(sep)]Cl_3 \cdot H_2O$ structures, there is evidence to suggest that the former may occur. Molecular energy minimizations of the conformations observed in these structures[19] indicate that the flattening of the caps can result entirely from the steric constraints within the cages, with possibly a minor contribution from electrostatic attraction between the N(cap) nitrogens and the positively charged CoN_6 chromophore. A similar steric argument has been proposed for the almost planar geometry about the tertiary nitrogen in the structure[20] of $P(OCH_2CH_2)_3N$, where the C–N–C angle is 119.7°. The increased planarity in this structure is associated with a further reduction of the N(cap)–C bond distance (to 1.425 (9) Å). This would be a natural deduction from the bonding mechanism suggested for the trigonal caps of the $[Co(sep)]^{2+/3+}$ structures.

Discussion

The possibility of encapsulation arose from a consideration of condensation reactions between aldehydes and amines coordinated to cobalt(III). Endo[21] and exo[22] imine products of the type I and II were shown to be extraordinarily stable in acid solution and

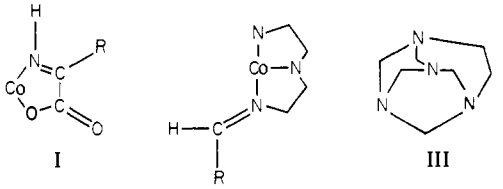

I II III

yet susceptible to attack by nucleophiles at the imine carbon atom. The reaction of the $[(en)_2CoC_2O_4]^+$ ion, for example, with formaldehyde in basic solution gave the dioxacyclam macrocyclic complex[23] in Scheme I.

The implication in such a synthesis is that the carbinolamines and related imines that are formed subsequently self-condense to give the cyclic ligand without rupture of any metal–ligand bonds. Activation of the coordinated imine toward nucleophiles could be expected since the metal ion substitutes for a proton, albeit not as well, in promoting nucleophilic attack. The imine coordinated to Co(III) therefore is intermediate in reactivity between the base imine and iminium ion. It is partly activated to nucleophiles and yet protected from protonation that leads to rupture of the imine. These properties along with some ancient organic chemistry involving the self-condensation of NH_3 and CH_2O to yield "hexamine" indicated how a tris bidentate amine might be capped to yield a cage.

The reaction betweren $[Co(en)_3]^{3+}$, CH_2O, and NH_3 led to a macrobicyclic complex in which the ligand completely encapsulates the cobalt ion. In keeping with the cryptate nomenclature, it has been given the trivial name cobalt(III) sepulchrate. The details

(16) Barnet, M. T.; Craven, B. M.; Freeman, H. C.; Kinie, N. E.; Ibers, J. A. *Chem. Commun.* **1966**, 307.
(17) Mak, T. C. W.; Lau, O. W.; Ladd, M. F. C.; Povey, D. C. *Acta Crystallogr., Sect. B* **1978**, *B34*, 1290.
(18) "International Tables for X-ray Crystallography"; Kynoch Press: Birmingham, England, 1968; Vol. III.
(19) Geue, R. J.; Sargeson, A. M., to be published.
(20) Clardy, J. C.; Milbrath, D. S.; Verkade, J. G. *Inorg. Chem.* **1977**, *16*, 2135.
(21) Harrowfield, J. MacB.; Sargeson, A. M. *J. Am. Chem. Soc.* **1974**, *96*, 2634.
(22) Gainsford, A. R.; Snow, M. R.; Springborg, J.; Taylor, D., to be published.
(23) Geue, R. J.; Snow, M. R.; Springborg, J.; Herlt, A. J.; Sargeson, A. M.; Taylor, D. *J. Chem. Soc., Chem. Commun.* **1976**, 285.

Scheme II

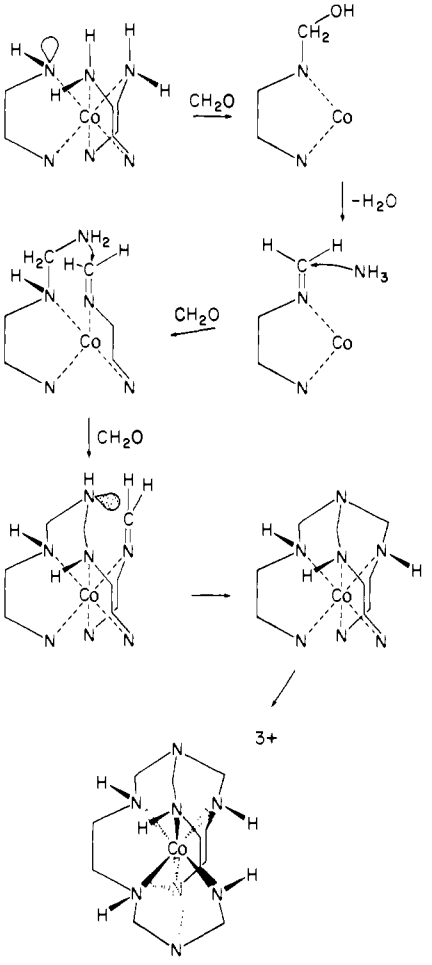

of the proposed synthetic route are shown in Scheme II.

The condensation of CH_2O with a bound deprotonated amine to give the coordinated carbinolamine is followed by elimination of H_2O.[21] The resultant imine is then attacked by NH_3 to yield the *gem*-diamine. Addition of another formaldehyde molecule and imine formation allows intramolecular condensation of the *gem*-diamine with the imine, and the first six-membered ring system is formed. Formation of another imine followed by intramolecular condensation of the secondary amine leads to the completed cap, and the process is repeated on the opposite octahedral face to give the completely encapsulated metal ion. The usual organic condensation between CH_2O and NH_3 is taking place simultaneously but by using a continuous supply and an excess of these reagents, the sepulchrate can be synthesized in large yields calculated with respect to the tris(ethylenediamine)cobalt(III) complex.

When samples were taken out and analyzed at different times during the reaction, intermediates of partly capped complexes were found, among others the complex with a $N(CH_2)_3$ cap at one end only. This compound has been called $[Co(semisepulchrate)]^{3+}$ and will be further described in a later publication.

Once the mechanism of the capping process is understood, strategies for the synthesis of a variety of complex cages become obvious and several have been carried out. Complexes of the 1,1,1-tris(((2-aminoethyl)amino)methyl)ethane (sen) ligand can be capped with the NH_3 and CH_2O reagents to yield the cobalt(III) tris(methyleneamine) capped sen complex $[Co(azamesar)]^{3+}$, but clearly any nucleophile with trigonal symmetry could be used, and some reactions of this type will be described in a later publication.

In addition to encapsulation, the $[Co(sen)]^{3+}$ ion also undergoes methylation. One of the products isolated has an extra C atom, and its ^1H NMR spectrum has features similar to the parent

Scheme III

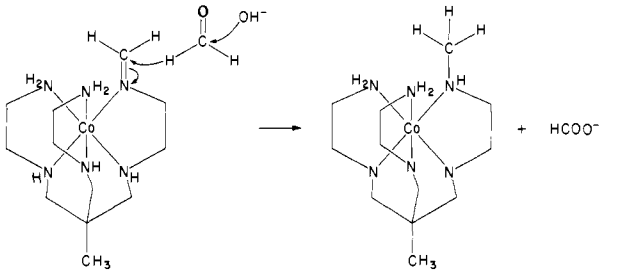

molecule, plus signals that could be attributed to an additional methyl group. In 3 M DCl, the complex is characterized by a singlet (3 H) at 1.0 ppm, a complex multiplet region between 2.1 and 3.3 ppm, plus a doublet at 2.3 ppm (21 H). The singlet correlates with CH_3 attached to tertiary C, the multiplet region with the complex signals expected for the methylene protons, and the doublet is assigned to methylation of a terminal NH_2 group. Methylation at a secondary N center would have led to a singlet.

Methylation presumably comes about by reduction of the carbinolamine formed from condensation of formaldehyde and $[Co(sen)]^{3+}$ as a result of a type of Canizzaro reaction, Scheme III. Similar alkylations have been observed with other metal systems and at the secondary N atoms of the cage, and these will be reported subsequently.

The isolation of only one isomer of $[Co(sep)]^{3+}$ appears rather extraordinary when the potential complexity of the stereochemistry is examined. There are seven chiral centers, the six bound N atoms and the metal ion. Superficially, there appear to be 2^6 possible isomers. However, some of these are degenerate, and there are only 16 unique species.[24] The apparently surprising stereospecificity can be accounted for by an examination of the stereochemistry of the complex ion and the mechanism of the synthesis in detail.

After the formation of the first *gem*-diamine and the generation of the second bound imine center, it can be seen in Scheme II that the chiral N center must be oriented so that the amine methene group is apical and the proton is equatorial before intramolecular cyclization to give the first six-membered ring can occur. This apical orientation of the six-membered chelate must then be maintained after the formation of the third imine center to complete the cap. Once formed, a model will show that the proton and $-CH_2-$ positions cannot be inverted, and the orientation of the Tris chelates decides the same configuration for all six chiral N centers. The Λ configuration[25] generates the *S* configuration at the N centers. The cage is very tight with little flexibility except the prospect of a total conformational change about the C_3 axis that converts all ethane-1,2-diamine conformations synchronously from λ to δ (*ob* to *lel*), where the *lel* and *ob* nomenclature[25] indicates the C–C axes parallel or oblique to the C_3 axis of the ion. At the same time, the configurations about Co and N are retained.

The crystal structure[2] confirms the hexadentate nature of the capsule with the tris(methyleneamine) cap added at both ends of the parent ion. The ethane-1,2-diamine rings have the *lel* conformation, and the overall symmetry is very close to D_3. The Λ and Δ nomenclature has been used for the cages by analogy with $[Co(en)_3]^{3+}$.

The same symmetry or rapid interconversion of the conformers is suggested in solution by the ^1H and ^{13}C NMR spectra. Only two ^{13}C signals (+0.389 and −13.245 ppm relative to 1,4-dioxane) are observed, one due to the ethane-1,2-diamine C atoms, the other due to the methene C atoms of both caps, equal in intensity. The proton spectra display AB doublet pairs for the cap methene groups and a more complex AA′BB′ pattern for the ethane-1,2-diamine protons.

(24) It was realized later that some of these possibilities were degenerate, but R. Tapscott first pointed out to us that there were 16 unique forms.
(25) *Inorg. Chem.* **1970**, *9*, 1.

Table XI. Circular Dichroism Data for Some Related Complexes

complex	λ, nm	$\Delta\epsilon_{max}$	ref
$\Lambda(+)_D$-$[Co(en)]^{3+}$	490	+1.89	29
	430	−0.17	
$\Lambda(-)_D$-$[Co(sen)]^{3+}$	502	+0.42	3b
	450	−1.05	
$\Lambda(-)_D$-$[Co(azamesar)]^{3+}$	463	−3.10	
	346	+0.561	
$\Lambda(-)_D$-$[Co(sep)]^{3+}$	461	−2.37	
	352	+0.983	

The absorption, rotary dispersion, and circular dichroism curves are characteristic of chiral Co(III) hexamine type complexes although the charge-transfer band is shifted to longer wavelengths.[26] However, the structural study requires the complex ion to have the same configuration $\Lambda(S)$ for the structure derived from Λ-$[Co(en)_3]^{3+}$ even though the CD and RD curves for the two complexes are essentially catoptric around 500 nm. This is predicted[27] by calculations based on the optical activity models of Richardson.[28] In the parent Λ-$[Co(en)_3]^{3+}$ ion, the positive band for the first ligand-field band (Table XI) has been ascribed to the dominance of the rotary strength for the $A_1 \rightarrow E(+)$ transition over the $A_1 \rightarrow A_2(-)$ transition in the D_3 ion.[29] We presume therefore that the relative rotary strengths are reversed for the caged molecule, and the A component is now stronger than the E. Uniaxial single-crystal circular dichroism at room temperature[30] shows this to be the case since the E component with positive CD is now observed. However, the problem is much more complicated in the single-crystal study, and this work has been published separately.[30]

The point is illustrated further by studying the effects of stepwise capping of Λ-$[Co(en)_3]^{3+}$ on the circular dichroism in solution (Table XI). In $(-)_D$-$[Co(sen)]^{3+}$, which can be envisaged as being $[Co(en)_3]^{3+}$ capped at one end and which can be regarded as having the Λ configuration,[31] the rotary strength of the first positive band is much reduced compared to that of Λ-$[Co(en)_3]^{3+}$. A similar effect has been observed on the addition of phosphate ion[29] to Λ-$[Co(en)_3]^{3+}$, where PO_4^{3-} supposedly sits on the C_3 axis and effectively caps it. Capping Λ-$[Co(sen)]^{3+}$ with NH_3 and CH_2O gives the complex $\Lambda(-)_D$-$[Co(azamesar)]^{3+}$. This yields a further reduction of the overall rotary strength of the first ligand-field band such that it becomes negative. The signs and magnitude of the bands are now similar to those observed for Λ-$[Co(sep)]^{3+}$.

The phenomena can be looked at as variations in the magnitude and position of the CD bands for the A and E components in these complexes, assuming an effective D_3 symmetry. As the capping occurs, the negative A component becomes dominant and it lies at somewhat higher energies than the E component. The positive and negative wings observed can then be ascribed to incomplete cancellation of the A and E components of opposite sign. Overall, the CD essentially changes sign as the capping progresses and as the configuration of the tris(en) chelate moiety remains the same.

The visible spectrum of the Co(II) ion is very similar to that of the parent high-spin $[Co^{II}(en)_3]^{2+}$ ion measured in the crystal lattice,[32] and the differences are no more than those observed between solution and solid-state spectra for the same ion. The measured magnetic moments for $[Co^{II}(sep)]^{2+}$ of 4.72 and $[Co^{II}(azamesar)]^{2+}$ of 4.56 μ_B are typical for high-spin Co(II) and essentially the same as for $[Co^{II}(en)_3]SO_4$ (4.65 μ_B).[33]

The stability of $[Co^{II}(sep)]^{2+}$, formed by reduction with Zn, to exchange and racemization is extraordinary. Although Co(II) complexes are usually labile, exchanging their ligands on a microsecond scale,[34] it was observed that chiral $[Co(sep)]^{2+}$ showed no loss of activity in 2 h. This inertness presumably arises from the tight helical packing of the ligand strands around the metal ion preventing it from dissociating. This was confirmed from the result that no exchange (<0.1%) between $^{60}Co_{aq}^{2+}$ and $[Co^{II}(sep)]^{2+}$ took place over a day at 25 °C. The tight packing also confers chiral stability on the $[Co(sep)]^{2+}$ since all seven chiral centers have to invert synchronously in order to racemise the complex.

The kinetic inertness and optical stability of the $[Co(sep)]^{2+}$ ion allows some interesting experiments to be carried out. Of special interest are electron-transfer studies, and these types of inert, chiral complexes lend themselves to the study of electron self-exchange by a simple method.[6] In mixing a chiral form of one oxidation state with the catoptric form of the other, i.e.,

$$\Lambda\text{-}[Co(sep)]^{2+} + \Delta\text{-}[Co(sep)]^{3+} \rightleftarrows \Lambda\text{-}[Co(sep)]^{3+} + \Delta\text{-}[Co(sep)]^{2+}$$

a change in rotation occurs, but there is residual rotatory power since the RD spectra are different for the two oxidation states. If electron transfer occurs between the two ions, then the mixture racemizes, provided the concentration of the two oxidation states is equal. The measured rate constant in this instance is $\sim 10^5$-fold faster than that for $[Co(en)_3]^{2+/3+}$ and $\sim 10^7$-fold faster than that for $[Co(NH_3)_6]^{2+/3+}$. This is very surprising considering the fact that the electronic states of the corresponding pairs of complexes are so similar and the metal ion is surrounded by a saturated insulating coat.

Arguments[35] accounting for the slow-electron-transfer reactions in Co(II)–Co(III) amine systems have often incorporated the restrictions arising from forbidden-spin-state changes and the Franck–Condon principle. For example, in the $[Co(en)_3]^{2+/3+}$ exchange, the $(t_{2g})^5(e_g)^2$ configuration of Co(II) is argued to convert to the $(t_{2g})^6(e_g)^1$ configuration before rapid electron transfer can ensue with the Co(III) $(t_{2g})^6(e_g)^0$ configuration.[38] Either there is a substantial activation barrier to the spin-state change or the equilibrium concentration of the low-spin Co(II) state is very low. Support for these proposals was adduced from the more rapid electron transfer observed in the stronger ligand-field complexes like $[Co(phen)_3]^{2+/3+}$ (~ 8 M^{-1} s^{-1}).[36] Here it is known that the $[Co(phen)_3]^{2+}$ ion is much closer to the high–low spin-crossover point,[37] and the concentration of the low-spin $(t_{2g})^6(e_g)^1$ state is therefore higher. Experimental support for slow spin-state changes in the ground state is lacking however, and it appears from the experiments that have been done on this problem that such changes occur in the nanosecond region.[38] The problem that has arisen from the cage chemistry is that the $[Co(phen)_3]^{2+/3+}$ and the $[Co(sep)]^{2+/3+}$ electron-transfer rates are very similar even though the caged ions appear to be no nearer the spin-crossover point than the parent $[Co(en)_3]^{3+/2+}$ system.

Crystallographic investigations of the $[Co^{III}(sep)]^{3+}$ and $[Co^{II}(sep)]^{2+}$ ions show Co–N bond lengths of 1.99[2] and 2.16 Å, respectively, whereas the $[Co(NH_3)_6]^{3+/2+}$ values are 1.97[39] and 2.16 ± 0.01 Å.[15] Clearly, these bond lengths do not differ greatly from those of the caged ions. It looks as if the spin-state restrictions and bond-length arrangements make a smaller contribution to the barrier for electron transfer than has been normally accepted, and we need to look elsewhere for the major component.

One explanation that could be offered is that the cage chemistry is normal and the $[Co(en)_3]^{2+/3+}$ and $[Co(NH_3)_6]^{2+/3+}$ rates are

(26) Saito, Y. *Top. Stereochem.* **1978**, *10*, 95 and references therein.
(27) Geue, R. J., to be published.
(28) Richardson, F. S. *J. Phys. Chem.* **1971**, *75*, 692. Richardson, F. J.; Caliga, D.; Hilmes, G.; Jenkins, J. J. *Mol. Phys.* **1975**, *30*, 257.
(29) Mason, S. F. *Q. Rev., Chem. Soc.* **1963**, *17*, 20 and references therein. Mason, S. F.; Norman, B. J. *J. Chem. Soc. A* **1966**, 307.
(30) Dubicki, L.; Ferguson, J.; Geue, R. J.; Sargeson, A. M. *Chem. Phys. Lett.* **1980**, *74*, 393.
(31) Reference 3 and Urbach, F., private communication.
(32) Yang, M. C.; Palmer, R. A. *J. Am. Chem. Soc.* **1975**, *97*, 5390.
(33) Datta, S. *Philos. Mag.* **1934**, *17*, 585. The literature gives values for the $[Co(en)_3]^{2+}$ ion ranging from 3.9 to 5.4 BM. The value selected here was adjudicated as a magnetic-dilute example (by: Lewis, J.; Figgis, B. *Prog. Inorg. Chem.* **1964**, *6*, 189) and was measured under comparable conditions to that for the cages.
(34) Eigen, M.; Wilkins, R. G. *Adv. Chem. Ser.* **1965**, *No. 49*, 55.
(35) See: *Discuss. Faraday Soc.* **1960**, *29*, 113. Basolo, F.; Pearson, R. G. "Mechanisms of Inorganic Reactions"; Wiley: New York, 1967; Chapter 7. Stynes, H. C.; Ibers, J. A. *Inorg. Chem.* **1971**, *10*, 2304.
(36) Baker, B. R.; Basolo, F.; Neumann, H. M. *J. Phys. Chem.* **1959**, *63*, 371.
(37) Judge, J. S.; Baker, W. A. *Inorg. Chim. Acta.* **1967**, *1*, 68.
(38) Binstead, R. A.; Beattie, J. K.; Dewey, T. G.; Turner, D. H. *J. Am. Chem. Soc.* **1980**, *102*, 6442.
(39) Iwata, M. *Acta Crystallogr., Sect. B* **1977**, *B33*, 59.

Scheme IV

$$[Co(sep)]^{2+} + O_2 \underset{}{\overset{RDS}{\rightleftharpoons}} [Co(sep)]^{3+} + O_2^{-}\cdot$$

$$2H^+ + O_2^{-}\cdot + [Co(sep)]^{2+} \xrightarrow{fast} [Co(sep)]^{3+} + H_2O_2$$

OR

$$2H^+ + 2O_2^{-}\cdot \xrightarrow{fast} H_2O_2 + O_2$$

abnormal. This could arise if the $[Co^{II}(en)_3]^{2+}$ ion was substantially in a monodentate form that did not undergo electron transfer with the $[Co(en)_3]^{3+}$ ion. In this way an electron-transfer rate comparable with that in the cage chemistry could be tolerated, provided the tris chelate Co(II) ion was $\sim 10^5$-fold less stable than the monodentate form. However, stability constant studies with $[Co(NH_3)_n]^{2+}$ ions indicate that $[Co(NH_3)_5(OH_2)]^{2+}$ is about 5-fold more stable than $[Co(NH_3)_6]^{2+}$ in 1 M NH_3.[9] It follows that the "chelate effect"[40] would require a smaller difference for the bidentate species, and this explanation therefore becomes untenable. These electron-exchange studies will be the subject of subsequent papers and are not pursued further here other than to say that molecular mechanics calculations on the ions indicate that the cage "hole size" may be a little too large for Co(III) and too small for Co(II).[27] Such effects would generate strain that could be relieved in the transition state, but it is evident that the effects do not show up in Co–N bond lengths.

Another redox reaction involving $[Co(sep)]^{2+}$ is the quantitative reaction with O_2 to give H_2O_2. The reaction is surprisingly fast (k_2 = 43 M^{-1} s^{-1} at 25 °C) and quite unusual for a Co(II) complex. Such species usually react with O_2 to give Co(III) peroxo dimers[41] such as $[(NH_3)_5Co{-}O{-}O{-}Co(NH_3)_5]^{4+}$. However, in the case of the Co cage, the ligand is packed so tightly about the metal ion and the cages are so stable that the formation of the peroxo dimers is not possible. In fact, the ligand packing is so close that coordination of O_2 to the Co(II) center seems to be excluded. This implies an outer-sphere redox process to generate the superoxide ion as an intermediate that then reacts rapidly with another $[Co(sep)]^{2+}$ ion or disproportionates to H_2O_2 and O_2. The chemistry is analogous to that of $[Ru(NH_3)_6]^{2+} + O_2$,[42] but our efforts to detect the O_2^- ion have not been successful (Scheme IV). For example, we have attempted to observe the $O_2^{-}\cdot$ radical by ESR spectroscopy using flow techniques, and we have looked carefully at the effect of a large excess of $[Co^{III}(sep)]^{3+}$ on the rate of reduction of O_2 without observing any decrease.[43]

It has not been possible to remove the sep ligand from the Co(III) complex. It survives prolonged boiling in 12 M HCl. Treatment of $[Co(sep)]^{2+}$ with acid leads to rupture of the cage, giving Co^{2+}(aq) and the components from which the cage was formed. The decomposition probably takes place by protonation of the nitrogen atoms in the caps leading to a reversal of the capping process with the formation of a labile Co(II) imine complex that dissociates its ligands rapidly in the acid solution. It is clear from the rate law, however, that even in the $[Co^{II}(sep)]^{2+}$ ion, the apical N atoms are not very basic and still have a $pK_a < 0$.

The low basicity of the bridgehead N atom is rather surprising. Even after making allowance for the overall charge (3^+) and the effect of three methylene amine substituents, the pK_a of the protonated cap should not be less than zero. A provocative explanation has been suggested that[44] arises from the flattening of the configuration about the bridgehead atom displayed in the crystal structure. Superficially, it could be argued that such a flattening would give the lone pair of electrons more p character and thereby make them more basic. However, the effect that such a flattening has on the stability of the protonated form is much more dramatic, and it appears from ab initio molecular orbital calculations that the latter effect dominates the issue and accounts for the low pK_a.

The formation of the $[Co(sep)]^{2+}$ complex opens up new areas of chemistry. Already we have prepared other caged Co complexes from $[Co(en)_3]^{3+}$ or $[Co(sen)]^{3+}$, HCHO, and reagents with labile hydrogen atoms. They differ widely in redox potentials (>0.6 V) and allow us to study redox reactions by reacting cages of different oxidation states with each other. This aspect will be addressed in a subsequent publication. Rhodium(III), iridium(III), and platinum(IV) ions have been encapsulated in this way, and this work will be published shortly. There is also a prospect of encapsulating other metal ions that are known to be labile to their coordination environment in solution, thereby making them kinetically inert. Clearly, this would lead to new systematic chemistry, and such goals are currently being pursued.

Acknowledgment. The support of the Danish Research Foundation, Dr. A. Ekstrom's assistance with the ^{60}Co experiments, and the results from the Australian National University Microanalytical Services Unit are all gratefully acknowledged.

Registry No. $[Co(sep)]Cl_3$, 71963-57-0; $[Co(sep)]ZnCl_4$, 71935-79-0; $[Co(sep)]S_2O_6{\cdot}H_2O$, 82837-73-8; [Co(azamesar)]Cl_3, 82769-64-0; Λ-[Co(azamesar)]Cl_3, 82796-44-9; Δ-[Co(azamesar)]Cl_3, 82796-45-0; [Co(*N*-Me(sen))]Cl_3, 82769-65-1; [Co(azamesar)]$ZnCl_4$, 82837-79-4; (±)-$[Co(en)_3]Cl_3$, 13408-73-6; (±)-[Co(sen)]Cl_3, 82796-46-1; $[Co(sep)]^{2+}$, 63218-22-4; Λ(*S*)-$[Co(sep)]^{2+}$, 82796-47-2; Δ(*R*)-$[Co(sep)]^{2+}$, 82837-80-7; Λ(*S*)-[Co(sep)]Cl_3, 82783-65-1; Λ(S)-$[Co(azamesar)]^{2+}$, 82769-66-2.

Supplementary Material Available: Tables of root-mean-square amplitudes of vibration of non-H atoms along principal axes of thermal ellipsoids and structure-factor amplitudes (12 pages). Ordering information is given on any current masthead page.

(40) Schwarzenbach, G. *Helv. Chim. Acta* **1952**, *35*, 2344.
(41) Fremy, E. *Liebigs Ann. Chem.* **1952**, *83*, 227.
(42) Pladziewicz, J. R.; Meyer, T. J.; Broomhead, J. A.; Taube, H. *Inorg. Chem.* **1973**, *12*, 639.
(43) Dubs, R. V., unpublished work.
(44) Nobes, R. H.; Pross, A.; Radom, L.; Sargeson, A. M., unpublished work.